



Protein dynamics detected in a membrane-embedded potassium channel using two-dimensional solid-state NMR spectroscopy

Christian Ader^a, Olaf Pongs^b, Stefan Becker^c, Marc Baldus^{a,*}

^a Bijvoet Center for Biomolecular Research, Utrecht University, Padualaan 8, 3584 CH Utrecht, The Netherlands

^b Universität Hamburg, Zentrum für Molekulare Neurobiologie, Institut für Neuronale Signalverarbeitung, Falkenried 94, 20251 Hamburg, Germany

^c Max-Planck-Institute for Biophysical Chemistry, Department for NMR-based Structural Biology, Am Fassberg 11, 37077 Göttingen, Germany

ARTICLE INFO

Article history:

Received 7 May 2009

Received in revised form 31 May 2009

Accepted 29 June 2009

Available online xxx

Keywords:

Dynamics

Ion channel

MAS

Membrane

Protein

Solid-state NMR

ABSTRACT

We report longitudinal ¹⁵N relaxation rates derived from two-dimensional (¹⁵N, ¹³C) chemical shift correlation experiments obtained under magic angle spinning for the potassium channel KcsA-Kv1.3 reconstituted in multilamellar vesicles. Thus, we demonstrate that solid-state NMR can be used to probe residue-specific backbone dynamics in a membrane-embedded protein. Enhanced backbone mobility was detected for two glycine residues within the selectivity filter that are highly conserved in potassium channels and that are of core relevance to the filter structure and ion selectivity.

© 2009 Elsevier B.V. All rights reserved.

1. Introduction

Protein dynamics play an essential role for molecular function [1] and nuclear magnetic resonance (NMR) has become a premier method to probe molecular dynamics at atomic resolution in solution [2,3]. For more than two decades (see, e.g., Ref. [4,5]), solid-state NMR (ssNMR) has provided spectroscopic means to study molecular structure and dynamics in a membrane environment where molecular size increases and protein structure is modulated by the presence of a surrounding bilayer matrix [6]. With recent advancements in the field of Magic-Angle-Spinning (MAS [7]) based ssNMR on membrane proteins (see, e.g., [8–10]), the structural analysis of larger membrane-embedded proteins becomes feasible.

For example, we have shown that for the chimeric KcsA-Kv1.3 potassium channel, ligand binding and channel inactivation can be studied at atomic level [11–14]. KcsA-Kv1.3 shares essential structural and functional features with the KcsA channel first identified in the gram-positive bacterium *Streptomyces lividans* [15]. KcsA has been characterized by a variety of structural and biophysical techniques and high resolution structural information is available [16–18]. The selectivity filter which entails the channel's high K⁺ selectivity and specificity [19] constitutes an essential part of the K⁺ channel and is highly conserved among potassium channels. During pH-induced activation KcsA and KcsA-Kv1.3 channels rapidly inactivate. The inactivation is

correlated with a conformational change of the filter from a conductive to a 'collapsed' conformation which renders potassium binding sites inaccessible and thereby blocks the passage of potassium ions.

Crystal structures initiated a series of in-silico molecular-dynamics (MD) studies [20–25] that addressed the conformational flexibility in the selectivity filter for the selective conduction of potassium ions. The dynamical dependence between filter and permeant ion was referred to as breathing motion and linked to the fundamental mechanism of ion gating [25]. MD simulations evaluating the energetics related to different ion occupancies within the selectivity filter suggested a two state conduction pathway for the permeant ion [21,26,27]. This is supported by electron density profiles obtained for K⁺ and larger analogues like Rb⁺ located in the selectivity filter of KcsA [21,26,27]. Experiment and simulation showed that filter stability depends crucially on the presence of potassium [17,23,28–30]. Mutations in the selectivity filter and within its close proximity strongly affect stability and gating properties of the potassium channel [31–36], confirming that conformational dynamics of the selectivity filter and its molecular environment play an important role for channel gating [31,32,37–47].

In principle, ssNMR provides an experimental means to directly examine ion channel dynamics in a bilayer environment and in different functional states. Compared to solution-state NMR, ssNMR provides a more direct measure for internal mobility, as no overall tumbling of the molecule has to be considered. Moreover, spectral resolution is not determined by the micellar surrounding, instead the type and nature of the lipid bilayer can be readily varied granting insight into membrane effects on protein structure and dynamics (see, e.g., [48,49], Ader et al., in preparation). For KcsA-Kv1.3, previous

* Corresponding author.

E-mail address: m.baldus@uu.nl (M. Baldus).

dipolar ssNMR correlation spectra speak in favor of a well defined structure in a membrane setting [12]. Here, we probed ^{15}N nuclear spin relaxation times to obtain a more detailed view of KcsA-Kv1.3 backbone dynamics with particular attention to selectivity filter residues. Following pioneering work by Torchia et al. [50,51] and more recent studies [52,53] on solid-phase globular proteins, we show that two-dimensional ssNMR in combination with ^{15}N -edited relaxation filtered spectroscopy provides a promising means to probe channel backbone dynamics in lipid bilayers.

2. Material and methods

Protein expression, isotope-labeling and reconstitution in asolection liposomes were done as previously described [14]. The sample used for this study contained approximately 150 nmol (10 mg) uniformly (^{13}C , ^{15}N) labeled KcsA-Kv1.3. The protein to lipid ratio was 1:100 (mol/mol) and the water content of the sample was about 50% (w/w). Site-specific ^{15}N nuclear longitudinal relaxation rates (R_1) were measured using two-dimensional R_1 -edited (^{15}N , ^{13}C) correlation experiments. The corresponding pulse sequence is shown in Fig. 1 and was adapted from previous R_1 investigations [52,53] on a microcrystalline protein by incorporation of a SPECIFIC-CP [54,55] transfer step. As a result, the ^{15}N , ^{13}C heteronuclear correlation spectrum is dominated by N-C α correlations. All spectra were obtained at about 283 K and 12.5 kHz MAS using an 800 MHz instrument (Bruker Biospin Karlsruhe). The ^1H - ^{15}N cross polarization (CP) step employed a linear ramp (100 to 80% field strength) on the ^1H channel. The CP period was 0.75 ms and the ^{15}N field strength was set to 35 kHz. The 2.5 ms ^{15}N - ^{13}C CP step used a linear ramp on the ^{13}C channel and a ^{15}N field strength of about 34 kHz establishing SPECIFIC [54,55] transfer. ^1H decoupling was obtained by SPINAL64 [56] and continuous wave (CW) with a decoupling field of 83.3 kHz. Spectra were obtained for three spin-lattice relaxation times (5, 10, and 20 s). We acquired 176–560 scans for each of the 40 increments in t_1 . Maximum acquisition times in t_1 and t_2 were 4 ms and 10 ms, respectively. The total experimental time for the spectra analyzed was about 140 h. In order to minimize effects due to changes in CP-efficiencies over the course of the experiment, spectra were acquired in interleaved steps and added after the whole dataset was completed. Furthermore, we monitored CP-efficiencies in between individual two-dimensional (2D) experiments by acquiring 1D control spectra. During the course of data collection, we did not observe any sizable intensity changes in the ssNMR spectra. The average ^{15}N nuclear longitudinal relaxation rate of KcsA-Kv1.3 was measured by fitting the integrals of a series of 1D ^1H - ^{15}N cross polarization (CP) spectra with an additional spin-lattice relaxation time before detection. For the external magnetic field of 18.8 T we obtained an average relaxation rate of 0.024 s^{-1} measured at an effective temperature of 283 K. This value compares favorably to values found for a microcrystalline protein [52,53].

3. Results and discussion

As previously shown [14], KcsA-Kv1.3 residues Thr75, Gly77, and Gly79 are essential for binding K^+ ions in the selectivity filter. These

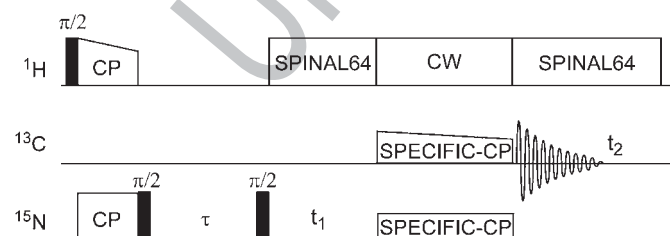


Fig. 1. Pulse sequence used to encode ^{15}N spin-lattice relaxation rates in ^{15}N - ^{13}C correlation spectra. All spectra were obtained at about 283 K and 12.5 kHz MAS.

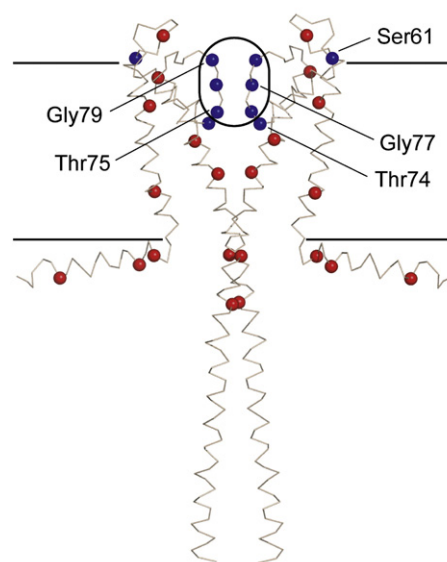


Fig. 2. Structural model for KcsA-Kv1.3 comprising residues 1–160 (only 2 subunits of the channel are shown) based on the crystal structure of full-length KcsA (PDB ID 3EFF) [18] and a full-length model based on EPR data for residues 1–24 (PDB ID 1F6G) [66]. Residues stated in the text and the following figures are labeled. Nitrogen atoms for which site-specific longitudinal relaxation rates (R_1) could be obtained are illustrated as blue spheres. Gly residues other than Gly77 and Gly79 are marked by red spheres. The selectivity filter of the potassium channel is marked by a black frame. The lipid bilayer is indicated by black lines.

residues can readily be resolved in N-C α correlation spectra. Our spectral analysis also included Thr74, close to the inner entrance of the filter, and Ser61, located in the turret region at the extra-cellular side of the KcsA-Kv1.3 channel (Fig. 2). Together with a set of α -helical Gly residues, several residue-specific probes were hence available for spectroscopic analysis (Figs. 2, 3). Obviously, the number of residues to be investigated could be increased by conducting NCACB [57] experiments, possibly even in three spectral dimensions. For reasons of spectroscopic sensitivity, such experiments were not attempted here.

In Fig. 3, we present relaxation-edited N-C α correlation spectra obtained for longitudinal ^{15}N delays of 5 and 20 s. Visual inspection of the spectra readily revealed a qualitative difference between residues Gly77 and Gly79, which occur at the upper, and Thr74 and Thr75, which occur at the lower part of the selectivity filter. Our data show

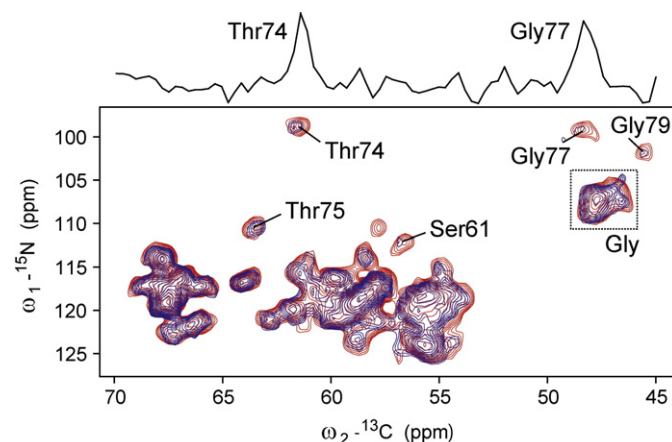


Fig. 3. Superposition of ^{15}N - ^{13}C correlation spectra obtained for membrane-embedded KcsA-Kv1.3 using ^{15}N spin-lattice relaxation delays of $\tau = 5\text{ s}$ (red) and $\tau = 20\text{ s}$ (blue). Resonances due to residues discussed in the text are labeled. The Gly N-C α region is marked by a dashed box. The slice on top was extracted from the spectrum employing $\tau = 5\text{ s}$ at a ^{15}N chemical shift of 99 ppm in order to illustrate signal-to-noise.

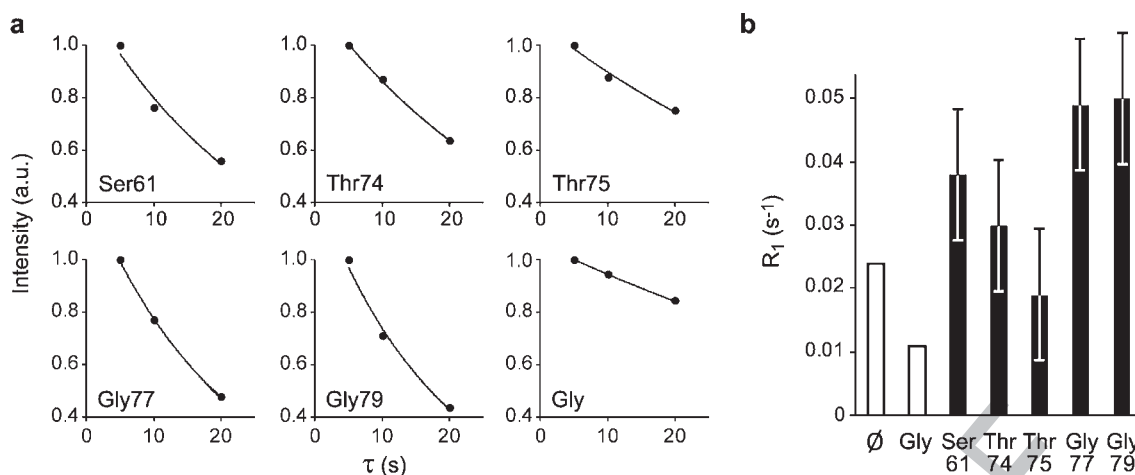


Fig. 4. (a) Decay curves measured for Ser61, Thr74, Thr75, Gly77, Gly79, and the Gly N-C α region. Corrected intensity values obtained for three relaxation delays ($\tau = 5, 10, \text{ and } 20$ s) were renormalized so that the data point for $\tau = 5$ s has an intensity value of 1. Solid curves give exponential fits to the data. (b) Bar graph summarizing the determined average (\emptyset) and site-specific ^{15}N spin-lattice relaxation rates.

151 that spin-lattice relaxation proceeds faster for Gly77 and Gly79 than
 152 for Thr74 and Thr75. In order to distinguish whether this observation
 153 originates from increased local mobility in the upper part of the
 154 selectivity filter or from larger motional freedom intrinsic for Gly
 155 residues, we included the Gly N-C α region (dashed box in Fig. 3)
 156 in our analysis. KcsA-Kv1.3 contains thirteen glycines per subunit,
 157 mainly located in helical segments of the KcsA-Kv1.3 channel (see
 158 Fig. 2). Subsequently, we determined peak volumes for the five
 159 resolved signals and the Gly region and subtracted noise levels by
 160 integrating and subtracting corresponding noise regions of the
 161 individual spectra in order to avoid systematic overestimation of
 162 small peak volumes obtained at long relaxation delays. In order to
 163 correct for different experiment times, we normalized peak volumes
 164 by the number of acquired scans. The resulting corrected peak
 165 integrals were standardized to the respective data point obtained for
 166 the relaxation delay of 5 s and data were fitted to an exponential decay
 167 in order to determine R_1 's (Fig. 4a). No correction for effects of magic
 168 angle spinning on R_1 and ^{15}N spin diffusion [52,53] was applied. Based
 169 on the signal-to-noise of our spectra, we estimate that our site-specific
 170 R_1 's are associated with an error of approximately 0.01 s^{-1} .

171 For residues Gly77 and Gly79 we measured ^{15}N backbone R_1 's of
 172 0.049 s^{-1} and 0.050 s^{-1} , respectively (Fig. 4b). These values are
 173 significantly larger than the average value obtained for KcsA-Kv1.3.
 174 Note other signals contributing to the Gly N-C α region are character-
 175 ized by comparatively slow relaxation rate of 0.011 s^{-1} , more than
 176 four times smaller than the relaxation rates obtained for the two Gly
 177 residues in the selectivity filter. On the other hand, we found ^{15}N
 178 backbone R_1 's of residues Thr74 and Thr75 of 0.03 s^{-1} and 0.019 s^{-1} ,
 179 respectively. The data suggest that increased mobility as observed for
 180 Gly77 and Gly79 is locally confined to the upper part of the selectivity
 181 filter. By contrast, Thr74 and Thr75 at the lower part of the selectivity
 182 filter have a local mobility similar to the average mobility in a channel
 183 backbone residue. In this context, it is interesting to note that
 184 mutation of Thr75 was not only found to change ion affinity but also
 185 substantially affected the thermal stability of the channel tetramer
 186 [33]. These findings suggest that this residue plays an important role
 187 for the integrity of the channel's quaternary structure in agreement
 188 with our finding that the lower part of the selectivity filter exhibits
 189 less backbone dynamics than the remaining filter segments. Finally,
 190 we determined a ^{15}N backbone R_1 of 0.038 s^{-1} for Ser61. This residue
 191 is located in the extra-cellular loop of KcsA-Kv1.3 and displays
 192 mobility above the protein's average. Nevertheless, the Ser61 value
 193 does not exceed T_1 rates observed for the Gly residues in the upper
 194 selectivity filter. The data is consistent with the idea that residues in
 195 the turret region are well structured in the resting state of the channel

196 at pH 7.5 [12] but likely exhibit higher molecular dynamics in the
 197 context of pH-induced gating [14].

198 On the basis of ^{15}N backbone R_1 's we have color coded in Fig. 5a the
 199 relative differences in local mobility observed for KcsA-Kv1.3 filter
 200 residues. For reference, selectivity filter residues affected by ligands
 201 which induce a distorted conductive (KTX, ref. [11,58]) or collapsed
 202 (porphyrin, Ref. [14]) backbone structure are indicated. Interestingly,
 203 filter residues identified as mobile are involved in both ligand binding
 204 modes. Next, we compared our results to crystallographic B-factors
 205 obtained for KcsA crystallized in the absence and presence of an FAB
 206 antibody (Fig. 5b, c). Neither of the two data sets shows qualitative
 207 agreement to our spectroscopic analysis. This disagreement may origi-
 208 nate from the different conditions in which the KcsA channel struc-
 209 tures were studied including parameters like pH, temperature, ionic
 210 strength, and lipid environment. The crystal structures for example
 211 were obtained using detergent solubilized KcsA, whereas ssNMR
 212 experiments utilize proteoliposome preparations. In fact, comparison
 213 of both X-ray data sets suggests that B-factors seem to depend mainly
 214 on the environment of the channel, i.e. residing in a free crystalline
 215 state or when bound to an FAB antibody.

216 Previously, solution-state NMR studies of KcsA variants were
 217 conducted at pH 7.5 in SDS micelles that revealed a molecular
 218 conformation comparable to the available crystal structures and
 219 allowed to examine ^{15}N relaxation rates as a quantitative measure of
 220 structural mobility [59,60]. These data suggested increased backbone
 221 mobility for the N- and C-terminal segments of closed KcsA and
 222 excluded backbone dynamics on the ps–ns time scale for selectivity
 223 filter residues at neutral pH. However, pH-induced gating could not be
 224 followed under such conditions. Instead, solution-state NMR of KcsA
 225 in DDM and foscoline micelles were used to gain insight in pH sensing
 226 and dynamics related to activation gating [61,62]. For example, Riek et
 227 al. followed structural dynamics of residue Y78 in the selectivity filter
 228 as a function of pH based on $^3\text{J}(\text{HN}, \text{H}\alpha)$ scalar couplings [61]. This
 229 data revealed millisecond timescale motions in the filter that were
 230 attributed to exchange between low and high K^+ affinity states.

231 On the other hand, we previously observed significantly larger
 232 structural changes after inactivation in lipid bilayers [14] compared to
 233 solution-state NMR studies. It suggests that protein dynamics are
 234 significantly different in a micellar versus a lipid bilayer environment.
 235 This is consistent with the idea that composition and mechanical
 236 status of the lipid bilayer have a profound influence on K^+ channel
 237 gating and stability, underlining the utility of ssNMR-based dynamic
 238 studies in a native or native-like membrane setting. Here, we showed
 239 the ^{15}N R_1 's are accessible for KcsA-Kv1.3 in a membrane setting
 240 revealing increased backbone dynamics in the upper selectivity filter

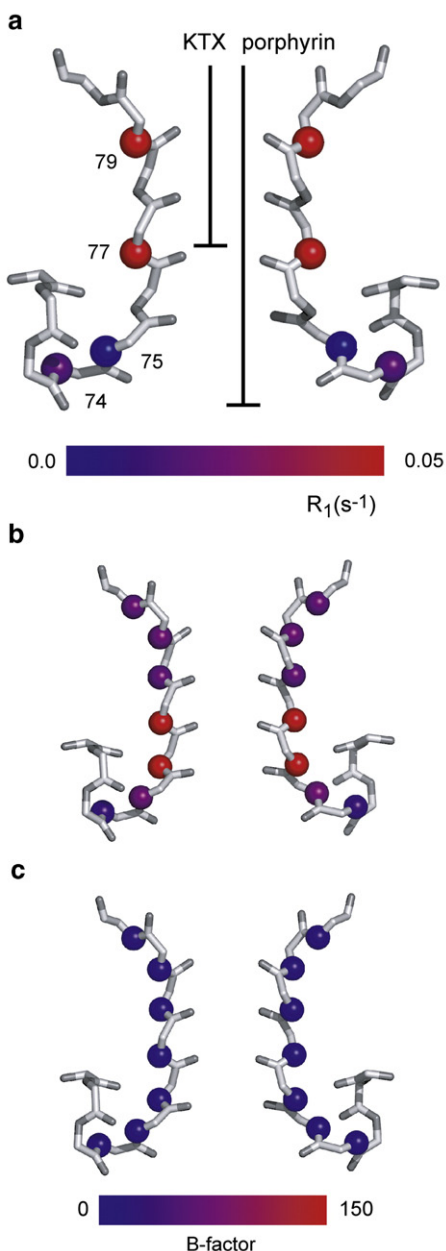


Fig. 5. (a) Selectivity filter of KcsA (PDB ID 1K4C) [17]. Backbone nitrogens for which R_1 's were determined are depicted as spheres. R_1 's are indicated by a color gradient from blue ($R_1 = 0.0 \text{ s}^{-1}$) to red ($R_1 = 0.05 \text{ s}^{-1}$). Bars indicate the residues affected by KTX and porphyrin binding, respectively. B-factors reported for backbone nitrogens of the selectivity filter and the two neighboring residues for KcsA crystal structures obtained in the absence (b, PDB ID 1BL8) [16] and presence (c, PDB ID 1K4C) [17] of FAB antibodies. B-factors are indicated by a color gradient from blue ($B = 0$) to red ($B = 150$).

of the closed channel at neutral pH. This approach may be used in the future to follow filter dynamics as a function of parameters such as pH or ion concentration controlling potassium channel function.

4. Conclusions

We have determined ^{15}N longitudinal relaxation rates for individual residues of KcsA-Kv1.3 in lipid bilayers. The experiments allow for a qualitative description of local backbone dynamics in the selectivity filter in reference to other segments of a membrane-embedded potassium channel. Site-specific R_1 's ranged from 0.019 s^{-1} to 0.050 s^{-1} at 18.8 T and the average protein backbone relaxation can be described by an overall rate of 0.024 s^{-1} . In absolute numbers, the values compare

favorably to data obtained on a crystalline protein at different magnetic fields. Our experiments confirm earlier conclusions based on dipolar ssNMR correlation spectroscopy [12] that KcsA-Kv1.3 resides in a well defined structure in a membrane setting. We observe a locally increased mobility for Gly77 and Gly79 in the upper part of the KcsA-Kv1.3 selectivity filter, while the Thr74 and Thr75 residues in the lower part display local dynamics similar to the average protein backbone. The two glycine residues are highly conserved in the pore of K^+ channels and their conformational dynamics are of crucial importance to the filter structure and ion selectivity (see, e.g., Ref. [34,35]). Here, we found that these residues are also characterized by distinctly high backbone mobility. We propose that this mobility is an essential property of the filter to dynamically respond to the binding and unbinding of ions while they pass along the K^+ binding sites in the filter during ion permeation. Furthermore, conformational backbone plasticity of the selectivity filter may be critical for the gating transitions of the K^+ channel involving conductive and 'collapsed' filter conformations or the binding of ligands to the K^+ channel pore. The results underline that T_1 relaxation rates provide a powerful means to follow site-specific dynamics in larger membrane-embedded proteins by solid-state NMR. To further dissect dynamical details associated with K^+ channel function, site-resolved measurement of ^{15}N backbone dynamics may in the future be assisted by measurements of transversal protein relaxation rates [63] or by a more detailed analysis of ssNMR chemical shifts and cross-peak amplitudes as recently demonstrated for other membrane proteins [64,65].

Acknowledgements

This work was funded in part by NWO and the DFG. C.A. is supported by a Kekule fellowship of the Stiftung Stipendien-Fonds der Verband der Chemischen Industrie, Germany.

References

- [1] R.G. Smock, L.M. Gierasch, Sending signals dynamically, *Science* 324 (2009) 198–203.
- [2] D.D. Boehr, D. McElheny, H.J. Dyson, P.E. Wright, The dynamic energy landscape of dihydrofolate reductase catalysis, *Science* 313 (2006) 1638–1642.
- [3] A. Mittermaier, L.E. Kay, New tools provide new insights in NMR studies of protein dynamics, *Science* 312 (2006) 224–228.
- [4] J. Seelig, Deuterium magnetic-resonance – theory and application to lipid-membranes, *Q. Rev. Biophys.* 10 (1977) 353–418.
- [5] J. Herzfeld, A. Roufosse, R.A. Haberkorn, R.G. Griffin, M.J. Glimcher, Magic angle sample spinning in inhomogeneously broadened biological-systems, *Philos. Trans. R. Soc. Lond., Ser. B Biol. Sci.* 289 (1980) 459–469.
- [6] R.B. Gennis, *Biomembranes: Molecular Structure and Function*, Springer, New York, 1989.
- [7] E.R. Andrew, A. Bradbury, R.G. Eades, Nuclear magnetic resonance spectra from a crystal rotated at high speed, *Nature* 182 (1958) 1659.
- [8] M. Hong, Structure, topology, and dynamics of membrane peptides and proteins from solid-state NMR spectroscopy, *J. Phys. Chem. B* 111 (2007) 10340–10351.
- [9] N.J. Traaseth, K.N. Ha, R. Verardi, L. Shi, J.J. Buffry, L.R. Masterson, G. Veglia, Structural and dynamic basis of phospholamban and sarcolipin inhibition of Ca^{2+} -ATPase, *Biochemistry* 47 (2008) 3–13.
- [10] U.H.N. Dürr, L. Waskell, A. Ramamoorthy, The cytochromes P450 and b5 and their reductases—promising targets for structural studies by advanced solid-state NMR spectroscopy, *Biochim. Biophys. Acta Biomembr.* 1768 (2007) 3235–3259.
- [11] A. Lange, K. Giller, S. Hornig, M.-F. Martin-Eauclaire, O. Pongs, S. Becker, M. Baldus, Toxin-induced conformational changes in a potassium channel revealed by solid-state NMR, *Nature* 440 (2006) 959–962.
- [12] R. Schneider, C. Ader, A. Lange, K. Giller, S. Hornig, O. Pongs, S. Becker, M. Baldus, Solid-state NMR spectroscopy applied to a chimeric potassium channel in lipid bilayers, *J. Am. Chem. Soc.* 130 (2008) 7427–7435.
- [13] C. Ader, R. Schneider, K. Seidel, M. Etzkorn, S. Becker, M. Baldus, Structural rearrangements of membrane proteins probed by water-edited solid-state NMR spectroscopy, *J. Am. Chem. Soc.* 131 (2009) 170–176.
- [14] C. Ader, R. Schneider, S. Hornig, P. Velisetty, E.M. Wilson, A. Lange, K. Giller, I. Ohmert, M.-F. Martin-Eauclaire, D. Trauner, S. Becker, O. Pongs, M. Baldus, A structural link between inactivation and block of a K^+ channel, *Nat. Struct. Mol. Biol.* 15 (2008) 605–612.
- [15] H. Schrempf, O. Schmidt, R. Kummerlen, S. Hinnah, D. Müller, M. Betzler, T. Steinkamp, R. Wagner, A prokaryotic potassium-ion channel with 2 predicted transmembrane segments from *Streptomyces-lividans*, *EMBO J.* 14 (1995) 5170–5178.
- [16] D.A. Doyle, J. Morais-Cabral, R.A. Pfuetzner, A. Kuo, J.M. Gulbis, S.L. Cohen, B.T. Chait,

- 324 R. MacKinnon, The structure of the potassium channel: molecular basis of K⁺
325 conduction and selectivity, *Science* 280 (1998) 69–77.
- [17] Y. Zhou, J.H. Morais-Cabral, A. Kaufman, R. MacKinnon, Chemistry of ion
326 coordination and hydration revealed by a K⁺ channel-Fab complex at 2.0 Å
327 resolution, *Nature* 414 (2001) 43–48.
- [18] S. Uysal, V. Vasquez, V. Tereshko, K. Esaki, F.A. Fellouse, S.S. Sidhu, S. Koide, E.
328 Perozo, A. Kossiakoff, Crystal structure of full-length KcsA in its closed
329 conformation, *Proc. Natl. Acad. Sci. U. S. A.* 106 (2009) 6644–6649.
- [19] R. MacKinnon, Potassium channels and the atomic basis of selective ion
330 conduction (Nobel lecture), *Angew. Chem., Int. Ed.* 43 (2004) 4265–4277.
- [20] T.W. Allen, S. Kuyucak, S.H. Chung, Molecular dynamics study of the KcsA
331 potassium channel, *Biophys. J.* 77 (1999) 2502–2516.
- [21] J. Aqvist, V. Luzhkov, Ion permeation mechanism of the potassium channel, *Nature*
332 404 (2000) 881–884.
- [22] S. Bernèche, B. Roux, Molecular dynamics of the KcsA K⁺ channel in a bilayer
333 membrane, *Biophys. J.* 78 (2000) 2900–2917.
- [23] L. Guidoni, V. Torre, P. Carloni, Potassium and sodium binding to the outer mouth
334 of the K⁺ channel, *Biochemistry* 38 (1999) 8599–8604.
- [24] I.H. Shrivastava, C.E. Capener, L.R. Forrester, M.S.P. Sansom, Structure and dynamics
335 of K channel pore-lining helices: a comparative simulation study, *Biophys. J.* 78
336 (2000) 79–92.
- [25] I.H. Shrivastava, M.S.P. Sansom, Simulations of ion permeation through a
337 potassium channel: molecular dynamics of KcsA in a phospholipid bilayer,
338 *Biophys. J.* 78 (2000) 557–570.
- [26] S. Bernèche, B. Roux, Energetics of ion conduction through the K⁺ channel, *Nature*
339 414 (2001) 73–77.
- [27] J.H. Morais-Cabral, Y. Zhou, R. MacKinnon, Energetic optimization of ion
340 conduction rate by the K⁺ selectivity filter, *Nature* 414 (2001) 37–42.
- [28] C. Domene, M.S.P. Sansom, Potassium channel, ions, and water: simulation
341 studies based on the high resolution X-ray structure of KcsA, *Biophys. J.* 85 (2003)
342 2787–2800.
- [29] S.W. Lockless, M. Zhou, R. MacKinnon, Structural and thermodynamic properties
343 of selective ion binding in a K⁺ channel, *PLoS Biol.* 5 (2007) e121.
- [30] Y. Zhou, R. MacKinnon, The occupancy of ions in the K⁺ selectivity filter: charge
344 balance and coupling of ion binding to a protein conformational change underlie
345 high conduction rates, *J. Mol. Biol.* 333 (2003) 965–975.
- [31] J.F. Cordero-Morales, L.G. Cuello, Y. Zhao, V. Jogini, D.M. Cortes, B. Roux, E. Perozo,
346 Molecular determinants of gating at the potassium-channel selectivity filter, *Nat.*
347 *Struct. Mol. Biol.* 13 (2006) 311–318.
- [32] J.F. Cordero-Morales, V. Jogini, A. Lewis, V. Vasquez, D.M. Cortes, B. Roux, E. Perozo,
348 Molecular driving forces determining potassium channel slow inactivation, *Nat.*
349 *Struct. Mol. Biol.* 14 (2007) 1062–1069.
- [33] M.N. Krishnan, P. Trombley, E.G. Moczydlowski, Thermal stability of the K⁺ channel
350 tetramer: cation interactions and the conserved threonine residue at the innermost
351 site (S4) of the KcsA selectivity filter, *Biochemistry* 47 (2008) 5354–5367.
- [34] F.I. Valiyaveetil, M. Leonetti, T.W. Muir, R. MacKinnon, Ion selectivity in a semi-
352 synthetic K⁺ channel locked in the conductive conformation, *Science* 314 (2006)
353 1004–1007.
- [35] F.I. Valiyaveetil, M. Sekedat, R. MacKinnon, T.W. Muir, Glycine as a D-amino acid
354 surrogate in the K⁺-selectivity filter, *Proc. Natl. Acad. Sci. U. S. A.* 101 (2004)
355 17045–17049.
- [36] M. Zhou, R. MacKinnon, A mutant KcsA K⁺ channel with altered conduction
356 properties and selectivity filter ion distribution, *J. Mol. Biol.* 338 (2004) 839–846.
- [37] S. Bernèche, B. Roux, A gate in the selectivity filter of potassium channels,
357 *Structure* 13 (2005) 591–600.
- [38] R. Blunck, J.F. Cordero-Morales, L.G. Cuello, E. Perozo, F. Bezanilla, Detection of the
358 opening of the bundle crossing in KcsA with fluorescence lifetime spectroscopy
359 reveals the existence of two gates for ion conduction, *J. Gen. Physiol.* 128 (2006)
360 569–581.
- [39] A.M.J. VanDongen, K channel gating by an affinity-switching selectivity filter, *Proc.*
361 *Natl. Acad. Sci. U. S. A.* 101 (2004) 3248–3252.
- [40] S. Chakrapani, J.F. Cordero-Morales, E. Perozo, A quantitative description of KcsA
362 gating I: Macroscopic currents, *J. Gen. Physiol.* 130 (2007) 465–478.
- [41] S. Chakrapani, J.F. Cordero-Morales, E. Perozo, A quantitative description of KcsA
363 gating II: Single-channel currents, *J. Gen. Physiol.* 130 (2007) 479–496.
- [42] L. Gao, X. Mi, V. Paajanen, K. Wang, Z. Fan, From the cover: activation-coupled
364 inactivation in the bacterial potassium channel KcsA, *Proc. Natl. Acad. Sci. U. S. A.*
365 102 (2005) 17630–17635.
- [43] L. Kiss, S.J. Korn, Modulation of C-type inactivation by K⁺ at the potassium channel
366 selectivity filter, *Biophys. J.* 74 (1998) 1840–1849.
- [44] H.T. Kurata, D. Fedida, A structural interpretation of voltage-gated potassium
367 channel inactivation, *Prog. Biophys. Mol. Biol.* 92 (2006) 185–208.
- [45] Y. Liu, M.E. Jurman, G. Yellen, Dynamic rearrangement of the outer mouth of a K⁺
368 channel during gating, *Neuron* 16 (1996) 859–867.
- [46] E.M. Ogielska, R.W. Aldrich, Functional consequences of a decreased potassium
369 affinity in a potassium channel pore. ion interactions and C-type inactivation,
370 *J. Gen. Physiol.* 113 (1999) 347–358.
- [47] J. Zheng, F.J. Sigworth, Selectivity changes during activation of mutant shaker
371 potassium channels, *J. Gen. Physiol.* 110 (1997) 101–117.
- [48] R. Mani, S.D. Cady, M. Tang, A.J. Waring, R.I. Lehrer, M. Hong, Membrane-
372 dependent oligomeric structure and pore formation of a β-hairpin antimicrobial
373 peptide in lipid bilayers from solid-state NMR, *Proc. Natl. Acad. Sci. U. S. A.* 103
374 (2006) 16242–16247.
- [49] J. Xu, U.H.N. Dürr, S.-C. Im, Z. Gan, L. Waskell, A. Ramamoorthy, Bicelle-enabled
375 structural studies on a membrane-associated cytochrome b5 by solid-state MAS
376 NMR spectroscopy, *Angew. Chem., Int. Ed.* 47 (2008) 7864–7867.
- [50] D.A. Torchia, Solid-state NMR-studies of protein internal dynamics, *Annu. Rev.*
377 *Biophys. Bioeng.* 13 (1984) 125–144.
- [51] H.B.R. Cole, D.A. Torchia, An NMR-study of the backbone dynamics of
378 staphylococcal nuclease in the crystalline state, *Chem. Phys.* 158 (1991) 271–281.
- [52] N. Giraud, A. Böckmann, A. Lesage, F. Penin, M. Blackledge, L. Emsley, Site-specific
379 backbone dynamics from a crystalline protein by solid-state NMR spectroscopy,
380 *J. Am. Chem. Soc.* 126 (2004) 11422–11423.
- [53] N. Giraud, M. Blackledge, M. Goldman, A. Böckmann, A. Lesage, F. Penin, L. Emsley,
381 Quantitative analysis of backbone dynamics in a crystalline protein from nitrogen-
382 15 spin-lattice relaxation, *J. Am. Chem. Soc.* 127 (2005) 18190–18201.
- [54] M. Baldus, A.T. Petkova, J. Herzfeld, R.G. Griffin, Cross polarization in the tilted
383 frame: assignment and spectral simplification in heteronuclear spin systems, *Mol.*
384 *Phys.* 95 (1998) 1197–1207.
- [55] A.T. Petkova, M. Baldus, M. Belenky, M. Hong, R.G. Griffin, J. Herzfeld, Backbone
385 and side chain assignment strategies for multiply labeled membrane peptides and
386 proteins in the solid state, *J. Magn. Reson.* 160 (2003) 1–12.
- [56] B.M. Fung, A.K. Khitrin, K. Ermolaev, An improved broadband decoupling
387 sequence for liquid crystals and solids, *J. Magn. Reson.* 142 (2000) 97–101.
- [57] M. Baldus, Correlation experiments for assignment and structure elucidation of
388 immobilized polypeptides under magic angle spinning, *Prog. Nucl. Magn. Reson.*
389 *Spectrosc.* 41 (2002) 1–47.
- [58] U. Zachariae, R. Schneider, P. Velisetty, A. Lange, D. Seeliger, S.J. Wacker, Y.
390 Karimi-Nejad, G. Vriend, S. Becker, O. Pongs, M. Baldus, B.L. de Groot, The molecular
391 mechanism of toxin-induced conformational changes in a potassium channel:
392 relation to C-type inactivation, *Structure* 16 (2008) 747–754.
- [59] J.H. Chill, J.M. Louis, J.L. Baber, A. Bax, Measurement of ¹⁵N relaxation in the
393 detergent-solubilized tetrameric KcsA potassium channel, *J. Biomol. NMR* 36
394 (2007) 123–136.
- [60] J.H. Chill, J.M. Louis, C. Miller, A. Bax, NMR study of the tetrameric KcsA potassium
395 channel in detergent micelles, *Protein Sci.* 15 (2006) 684–698.
- [61] K.A. Baker, C. Tzitzilonis, W. Kwiatkowski, S. Choe, R. Riek, Conformational
396 dynamics of the KcsA potassium channel governs gating properties, *Nat. Struct.*
397 *Mol. Biol.* 14 (2007) 1089–1095.
- [62] K. Takeuchi, H. Takahashi, S. Kawano, I. Shimada, Identification and characteriza-
398 tion of the slowly exchanging pH-dependent conformational rearrangement in
399 KcsA, *J. Biol. Chem.* 282 (2007) 15179–15186.
- [63] S.D. Cady, M. Hong, Amantadine-induced conformational and dynamical changes
400 of the influenza M2 transmembrane proton channel, *Proc. Natl. Acad. Sci. U. S. A.*
401 105 (2008) 1483–1488.
- [64] K. Seidel, O.C. Andronesi, J. Krebs, C. Griesinger, H.S. Young, S. Becker, M. Baldus,
402 Structural characterization of Ca²⁺-ATPase-bound phospholamban in lipid bilayers
403 by solid-state nuclear magnetic resonance (NMR) spectroscopy, *Biochemistry* 47
404 (2008) 4369–4376.
- [65] M. Etzkorn, H. Kneuper, P. Dunnwald, V. Vijayan, J. Kramer, C. Griesinger, S. Becker,
405 G. Uden, M. Baldus, Plasticity of the PAS domain and a potential role for signal
406 transduction in the histidine kinase DcuS, *Nat. Struct. Mol. Biol.* 15 (2008)
407 1031–1039.
- [66] D.M. Cortes, L.G. Cuello, E. Perozo, Molecular architecture of full-length KcsA: role
408 of cytoplasmic domains in ion permeation and activation gating, *J. Gen. Physiol.*
409 117 (2001) 165–180.